Available online at www.sciencedirect.com
SCIENCE DIRECT®
Icarus 176 (2005) 305–315
ICARUS
www.elsevier.com/locate/icarus

Cassini UVIS observations of Europa's oxygen atmosphere and torus

Candice J. Hansen [a,*], Donald E. Shemansky [b], A.R. Hendrix [a]

[a] *Jet Propulsion Laboratory, California Institute of Technology, Mail Stop 169-237, 4800 Oak Grove Dr., Pasadena, CA 91109-8099, USA*
[b] *Department of Aerospace Engineering, University of Southern California, 854 W. 36th Place, Los Angeles, CA 90089-1191, USA*

Received 17 April 2004; revised 1 February 2005

Available online 5 April 2005

Abstract

Observations of the Europa environment using the Cassini UltraViolet Imaging Spectrograph (UVIS) show the presence of an extended atomic oxygen atmosphere in addition to the bound molecular oxygen atmosphere first detected by Hubble Space Telescope in 1994 [D.T. Hall, D.F. Strobel, P.D. Feldman, M.A. McGrath, H.A. Weaver, 1995, Detection of an oxygen atmosphere on Jupiter's moon Europa, Nature 373, 677–679]. The atomic oxygen measurement provides a direct constraint on the sputtering and loss of Europa's water ice surface and the interaction of Europa's atmosphere with Jupiter's magnetosphere. We derive a loss rate for O_2 based on the emission rate of the OI 1356 Å multiplet. UVIS detected substantial variability in the oxygen emission from Europa's oxygen atmosphere that we attribute to the viewing geometry. B.H. Mauk, D.G. Mitchell, S.M. Krimigis, E.C. Roelof, C.P. Paranicas [2003, Energetic neutral atoms from a trans-Europa gas torus at Jupiter, Nature 421, 920–922] inferred the presence of a torus of neutral gas at Europa's orbit based on Cassini's energetic neutral atom (ENA) image of the Jupiter system acquired with the Magnetospheric Imaging Instrument (MIMI), with the most likely torus constituents being hydrogen and oxygen species sputtered from Europa. Cassini UVIS data rule out O and O_2 as the possible torus species reported by Mauk et al. however, unless the torus density is so low that it is undetectable by UVIS (less than 8 atoms/cm^3). The UVIS observations indicate the presence of atomic hydrogen and possibly other species, but a full analysis is deferred to a following paper. The hydrogen in the present observations shows a local-time asymmetry and complex spatial distribution.
Published by Elsevier Inc.

Keywords: Europa; Satellites, atmospheres

1. Introduction

The Cassini–Huygens spacecraft encountered Jupiter at a minimum range of 137 R_J on December 31, 2000, en route to its final destination at Saturn. The observation period extended from October 2000 through March 2001. The phase angle coverage and advanced technology of the Cassini instrument package provided significant advances over Galileo and earth-based observations of the Galilean satellites in spite of the large flyby distance.

Two lengthy UltraViolet Imaging Spectrograph (UVIS) observations of Europa were acquired in conjunction with Io torus observations. The original objective of the analysis of the UVIS Europa data was to confirm the Hall et al. (1995) detection of a tenuous oxygen atmosphere and to compare our data, acquired at a different time and different position of Europa in Jupiter's magnetosphere, to the Hubble Space Telescope (HST) results. The UVIS data are free of earth emissions that potentially complicate HST measurement interpretation. After the reported detection of a torus of energetic neutral atoms associated with Europa (Mauk et al., 2003) we expanded our analysis to characterize the Europa torus size, density and composition.

2. Europa observations

The UVIS spectrographs tracked the position of Europa for two observational periods, one extending for 17,000 s

* Corresponding author. Fax: +1 818 393 4619.
E-mail addresses: candice.j.hansen@jpl.nasa.gov (C.J. Hansen), dons@hippolyta.usc.edu (D.E. Shemansky), amanda.r.hendrix@jpl.nasa.gov (A.R. Hendrix).

0019-1035/$ – see front matter Published by Elsevier Inc.
doi:10.1016/j.icarus.2005.02.007

while Europa was on the anti-solar side of Jupiter and another extending for 41,000 s while Europa was on the sub-solar side. The data obtained during these periods are the basis of the present work. The image of Europa in the slits was held to within an estimated 0.1 mr during the observational period.

The first Europa/torus observation began at 0730 UTC on January 6, 2001 at a range of 11.2×10^6 km from Europa (11.8×10^6 km from Jupiter). The total duration of the observation was ∼ 4.7 h. The UVIS integration time during this period was 1000 s. Seventeen images were collected. The second observation began at 0630 UTC on January 12, 2001 at a range of 15.8×10^6 km from Europa (15.6×10^6 km from Jupiter). Forty-one 1000 s images were collected. The instrument setup was the same for both observations. The geometry is summarized in Table 1.

Table 1
Summary of the Europa observation geometry

	January 6, 2001	January 12, 2001
Range to Jupiter (km)	11.8×10^6	15.6×10^6
Jupiter sub-spacecraft latitude	−1.7°	−2.6°
Range to Europa (km)	11.2×10^6	15.8×10^6
Europa phase angle	94°	116°
Europa sub-spacecraft latitude	−2.1°	−2.8°
Europa sub-spacecraft longitude	201°–220° W	64°–103° W
Angular size of Europa	0.28 mr	0.20 mr
Individual integration periods	1000 s	1000 s
Total integration time	17,000 s	41,000 s
Observation duration	4.7 h	11.4 h

The Cassini UVIS instrument has a far ultraviolet (FUV) channel (1100 to 1800 Å) and an extreme ultraviolet (EUV) channel (550 to 1100 Å). We have concentrated on the FUV channel for analysis of Europa's atmosphere. The FUV has a choice of 3 slit widths, and for this observation the low resolution (1.5 mr) slit was selected. This gives the data a spectral resolution of 4.8 Å (McClintock et al., 1992; Esposito et al., in press). The 2-dimensional detector collects up to 1024 spectral pixels by 64 spatial pixels. The Europa data had full (single pixel, not binned) spectral and spatial resolution. The instantaneous field of view (IFOV) with the low resolution slit is 1.5 mr (spectral dimension) × 1.0 mr (spatial dimension). With this slit width six 0.25 mr pixels in the spectral dimension on the detector are illuminated.

The UVIS slit was oriented perpendicular to Jupiter's equatorial plane as shown in Fig. 1a. On January 6 Europa subtended an angle of 0.28 mr, thus was sub-pixel in size (straddling pixel 31 and 32) in the spatial dimension, and slightly larger than a pixel in the spectral dimension. The observation geometry from Cassini was quite different than

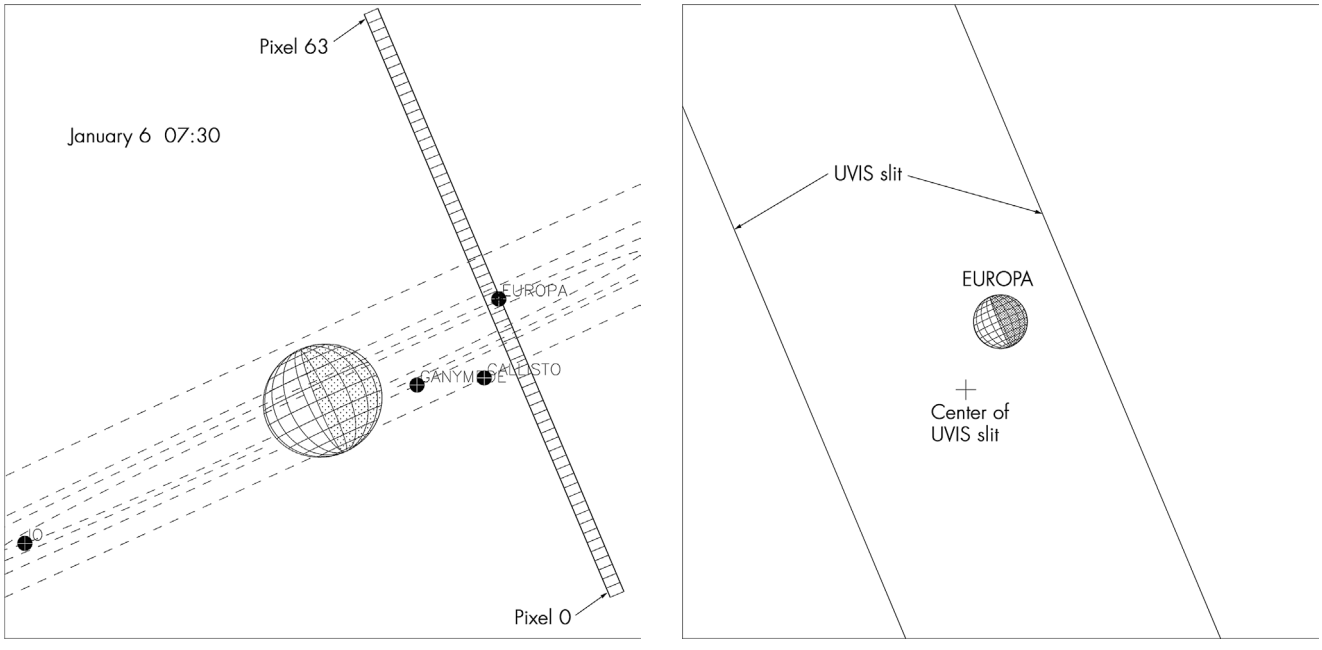

(a) (b)

Fig. 1. (a) This plot shows the position of Europa in its orbit near the beginning of the observation on January 6. The spatial dimension of the slit is oriented parallel to Jupiter's spin axis. The subspacecraft Jupiter latitude of −1.7° gives enough of an opening angle for UVIS to resolve both sides of Europa's orbit. Orbits of all the satellites are shown with dashed lines. The detector pixel size is 1 mr spatial × 0.25 mr spectral. The FUV spectral slit width is 1.5 mr. Each pixel depicted in this plot is 1.0 × 1.5 mr. The plot navigation is based on the post-flyby reconstructed spacecraft trajectory and spacecraft orientation. (b) At Cassini's range Europa is subpixel in the FUV slit (shown) in the spatial dimension, not spatially resolved, while being approximately the size of a pixel (0.28 mr diameter) in the spectral dimension. The image of Europa is split between row pixels 31 and 32. Europa is not centered in the UVIS slit because this observation was targeted to center Cassini's camera on Europa. This offset is maintained throughout the observation. Emission lines from Europa are shifted on the instrument spectral scale because of the off-center position and underfill of the planet image. (c) (1,2,3) On January 12 Europa was on the sub-solar side of Jupiter, near the ansa of its orbit as seen from the spacecraft. Over the course of the 11.4 h observation Europa moved from the far side through the ansa to the near side of its orbit as seen from Cassini.

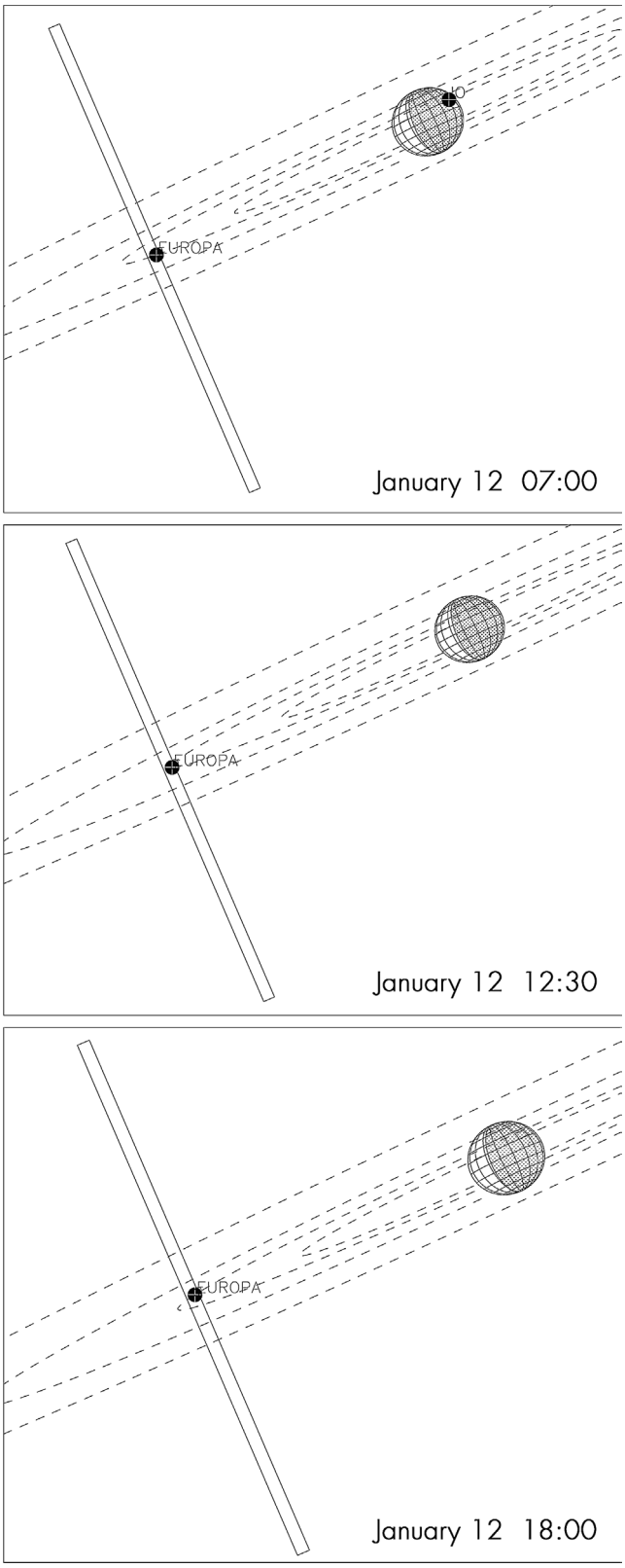

(c)

Fig. 1. Continued.

the view available to earth-based telescopes in that we could observe at $>90°$ phase angle, and see portions of both the leading and trailing sides of Europa.

The boresight selected for the targeting was the Cassini camera, which is offset 0.37 mr from the UVIS FUV, so Europa was positioned off-center, but still within, the slit for the duration of the observation, as shown in Fig. 1b. On January 12 Europa was on the day side of Jupiter, near the ansa of its orbit as seen from Cassini. During the January 12 observation Europa was tracked from the far side of its orbit, around the ansa to the near side over the duration of the observation, as illustrated in Fig. 1c(1,2,3).

Full spatial resolution perpendicular to Jupiter's equatorial plane allowed us to look for the Europa torus reported by Mauk et al. (2003). Mauk and co-workers postulated a torus radius of 1 to 5 R_j. The extent of a torus, if it had (for example) a diameter of 2 jovian radii, at the range at the time of the UVIS observation and opening angle of Europa's orbit, would be ~ 22 UVIS pixels, as can be seen in Fig. 1a.

3. Previous observations

Europa's oxygen atmosphere was first detected by Hall and co-workers in 1994 using the Goddard High Resolution Spectrograph (GHRS) on the Hubble Space Telescope (HST). More observations were acquired with HST in 1996 (Hall et al., 1998) and 1999 using the HST Space Telescope Imaging Spectrograph (McGrath et al., 2000, 2004), and Cassini imaged oxygen emission at visible wavelengths (Porco et al., 2003). Europa's water ice surface experiences charged particle bombardment and erodes due to sputtering and to a lesser extent sublimation (e.g., Johnson et al., 1981; Cheng et al., 1986; Shi et al., 1995; Ip, 1996; Johnson, 1996; Johnson and Quickenden, 1997, Shematovich et al., in preparation). Sputtered water products include H_2 and O_2. The H_2 is preferentially lost, leaving behind an atmosphere composed predominantly of O_2. Hall et al. (1995) observed atomic oxygen emission features at 1304 and 1356 Å and concluded that these were the signature of a bound O_2 atmosphere with a scale height of 20 to 300 km.

Hall and co-workers interpreted their spectrum as being predominantly due to O_2. The three most probable processes that produce the observed emissions are

(1) electron-impact excitation of oxygen atoms,
(2) electron-impact dissociative excitation of O_2, and
(3) resonance scattering of solar OI 1304 Å photons from oxygen atoms.

Using models for the charged particle environment experienced by Europa at 9.5 R_j in Jupiter's magnetosphere (Hall et al., 1998; Saur et al., 1998), Hall and co-workers derived the electron impact rates for processes (1) and (2). The ratio of electron impact rate coefficients for processes (1) and (2) yield distinctly different ratios for the 1356/1304 flux

ratios: 0.1 for electron-impact excitation of oxygen atoms, and 1.8 for electron-impact dissociative excitation of O_2. Hall and co-workers argued that the 1356/1304 flux ratio measured by HST was consistent with process 2, thus with O_2.

Using Cassini's Ion and Neutral Camera (INCA), which is a channel of the Magnetospheric Imaging Instrument (MIMI), an Energetic Neutral Atom (ENA) image was acquired during the Jupiter flyby (Mauk et al., 2003). The reduced ENA image peaks near Europa's orbit. Mauk and co-workers proposed an emission region with a radial extent and height of 1 to 5 Jupiter radii (R_J), symmetric about Europa's orbit, with a population of ∼40 atoms or molecules per cm^3 (assuming a torus radius of 2 Jupiter radii). This postulate is corroborated by the Energetic Particles Detector (EPD) instrument on the Galileo spacecraft measurement of a depletion of energetic particle flux in the vicinity of the orbit of Europa (Lagg et al., 2003). Mauk and co-workers were unable to say what the source composition of the torus is, but expected that sputtered ice products (O, O_2, H, H_2) would be the most likely constituents. A neutral population this high should have been detectable in the UVIS data so we analyzed the oxygen emission features at 1304 and 1356 Å to look for the presence of O and O_2 and evaluated the 1216 Å flux to look for hydrogen.

4. UVIS data analysis and discussion

4.1. Data processing steps

Fig. 2a shows the Europa FUV spectrum we obtained on January 6. All data has been summed over 4.7 h. Fig. 2b shows the segment of the spectrum between 1280 and 1380 Å with the 1304 (^3P–^3S_o) and 1356 (^3P–^5S_o) atomic oxygen emission features apparent in the raw data before the data was filtered and the fixed pattern signature (flat field) correction applied. The 1304 Å emission feature is a triplet of emissions at 1302.2, 1304.9, and 1306.0 Å and these lines are resolved in the raw UVIS spectrum. The 1356 feature is a doublet at 1355.6 and 1358.5 Å, also resolved in the UVIS spectrum. The fixed pattern noise in the data makes it difficult to pick out the individual lines, which is why all other plots show the data with the flat field correction applied. The fact that the individual lines are observed is indicative that Europa (and its atmosphere) is a point source smaller than the UVIS pixel, verified by running the Europa oxygen source through the instrument simulator as a point source and as an extended source. The offset of Europa from the center of the slit results in a spectral-channel shift of the spectrum, discussed in the next section.

In order to determine the precise flux attributable to the Europa oxygen atmosphere and potential torus, other features in the UVIS spectrum had to be accounted for and subtracted out. This includes the Io torus, the Local Interstellar Medium (LISM), the fixed pattern noise of the detector, reflected sun light, and the general background level including scattered light from these sources and Cassini's RTGs. We followed a very careful and deliberate process to isolate the signal due solely to Europa. The data was processed by pre-filtering with a 1-4-6-4-1 filter. A 1-4-6-4-1 filter assigns a value to each spectral pixel of $0.375x$ the pixel's value $+ 0.25x$ the two neighboring pixels' values $+ 0.0625x$ the values of the pixels two away from the central pixel being computed. This filter was selected to provide the optimal balance between improvement of statistics, suppression of noise, and minimization of filtering. Filtering was followed by flat-fielding based on a long integration LISM spectrum (162 h integration time) acquired by UVIS during cruise. Rows 50 to 56 in the Europa data were averaged to characterize the actual level of the LISM signal in the Europa spectrum. In Fig. 2c the flat-fielded spectrum for pixel 32 shows the analysis of each of the components of the spectrum, i.e. the background of the spectrum of Europa's atmosphere.

In order to establish the Io torus contribution to the Europa signal the spatial rows straddling Europa's position (29 and 30, 33 and 34) were averaged and compared to Europa's spectrum in spatial rows 31 and 32, as shown in Fig. 2d. There are no discernible emissions other than atomic oxygen and hydrogen attributable to Europa in this region of the spectrum.

Fig. 2d shows that once these contributions to the data are modeled the remaining peaks are the combined signal from Europa's oxygen atmosphere and reflected sunlight from Europa's surface. The 133.5 nm reflectance feature is marginally detected above the background. This relatively low signal compared to the HST observations (Hall et al., 1995) is consistent with the higher phase angle during the Cassini observation. The 133.5 nm feature was used to determine Europa's albedo at 94° phase angle (∼ 1%) and account for the reflected solar light contribution to Europa's spectrum at 1216, 1304, and 1356 Å, assuming the albedo is flat through this region of the spectrum. The solar spectrum is based on a high resolution solar spectral model developed by Shemansky, normalized to the TIMED_SEE data of October 2002. This step might be in error by 20% however it is 20% of a small number and does not affect our conclusions. A final subtraction of the reflected light leaves the signal due solely to Europa's atmosphere.

A similar process was used to analyze the hydrogen flux potentially coming from a Europa torus. Fig. 2e is a similar illustration scaled to show the hydrogen at 121.6 nm. The purple line on the plot shows the LISM flux. The green line shows H Lyman alpha (HLya) at the position of Europa indicating an excess over LISM.

Although not illustrated, the January 12 data set was processed by a similar series of steps. Since Europa was well away from the Io torus at the time of the January 12 observation the analysis was simpler.

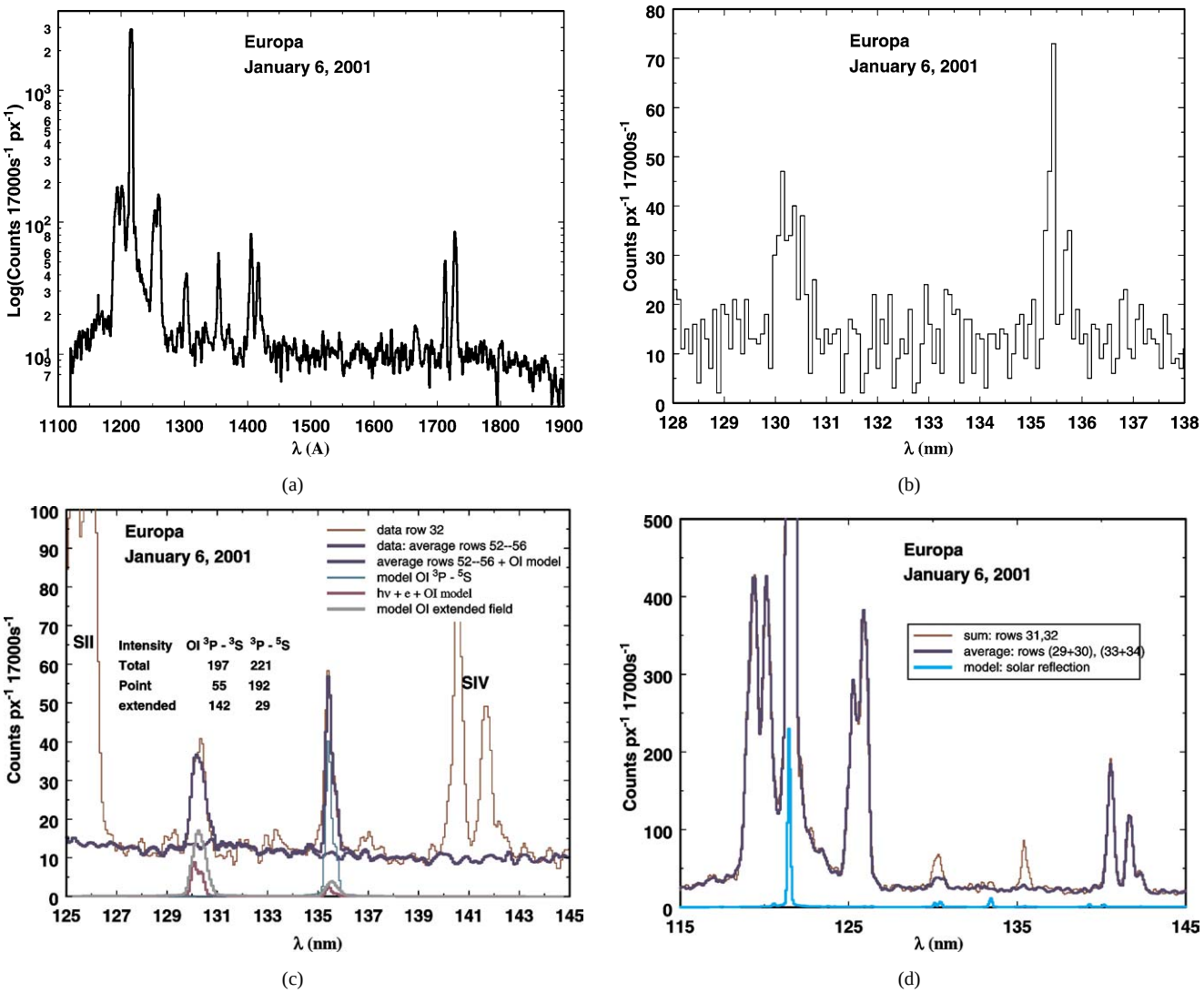

Fig. 2. (a) This is the full UVIS FUV spectrum, filtered and flat-fielded, acquired on January 6, summed over 4.7 h. The intensity scale is logarithmic to portray the full dynamic range. The Europa signal shows atomic oxygen emission at 1304 and 1356 Å. Other features in the spectrum are dominated by Io torus emissions in sulfur and LISM emission in the H Lya line. (b) This raw uncorrected segment of the Europa spectrum shows the oxygen emission multiplets at 1304 and 1356 Å. The 1304 Å emission feature is a triplet of emissions at 1302.2, 1304.9, and 1306.0 Å. The 1356 feature is a doublet at 1355.6 and 1358.5 Å. The UVIS is resolving the individual emission lines of the multiplets, consistent with observation of a point source. All other data illustrated in this paper has been smoothed using a 1-4-6-4-1 smoothing function. (c) The original spectrum and derived components are shown for the flat-fielded exposure for FUV row pixel 32. The flat field was generated using LISM data collected during cruise. The spectrum is a mix of shifted point source and filled field components. The location of the point source lines confirms the spacecraft pointing system position of the Europa image in the FUV aperture. The breakdown of point and spatially extended line components is shown quantitatively on the plot and in plotted simulated lines. The LISM background signal at the time of the observation was modeled using an average of pixels 52 to 56 (heavy blue). Along the bottom of the plot the best-fit model predicts for Europa oxygen emission features are shown. (d) The average of row pixel data 29, 30, 33, 34 superposed on the Europa row data to show the contribution of Io plasma torus emission after flat-fielding and LISM removal, illustrated with the dark blue line, which is the sum of pixel 31 and 32. The red spectrum shows the oxygen flux from Europa's sunlit surface and atmosphere at 1304 and 1356 Å. The weak solar reflection component is based on the reflected carbon feature at 1335 Å, which enabled determination of the albedo of Europa at 94° phase angle and subsequent calculation of the contribution of reflected sunlight to the 1304, 1356 and 1216 Å features, as illustrated with the turquoise line. (e) The H Lyα emission line spectrum at the Europa position is compared to the assumed LISM contribution at row pixels 50–56.

4.2. Europa's oxygen atmosphere

The determination of oxygen flux from the UVIS measurements is a two-step, iterative modeling process. The first step is a prediction of oxygen emission photons based on electron energies and densities in the jovian environment for one atom or molecule of oxygen per cm^3. The second step models the appearance of those emission features simulating the UVIS instrument response. The simulated line features are dependent on the assumed size and position of the source in the slit. The predicted spectrum is scaled to fit to the actual spectrum (which has been processed as described above) for final determination of oxygen flux and abundance.

Table 2
Rate coefficients used for emission features due to molecular oxygen, based on the experimental data of Kanik et al. (2003) and the two-component jovian energetic electron environment. Uncertainties in k are </= 15%

Process, wavelength (Å)	Rate coefficient, k ($cm^3\ s^{-1}$)	Electron temperature (K)	Electron density [e^-] (cm^{-3})	g-value (per second) $= k * [e^-]$
$e + O_2$(1356)	1.46E-09	2.3E5	40	5.83E-08
$e + O_2$(1356)	3.47E-09	2.3E6	4	1.39E-08
$e + O_2$(1304)	5.49E-10	2.3E5	40	2.19E-08
$e + O_2$(1304)	1.52E-09	2.3E6	4	6.07E-09

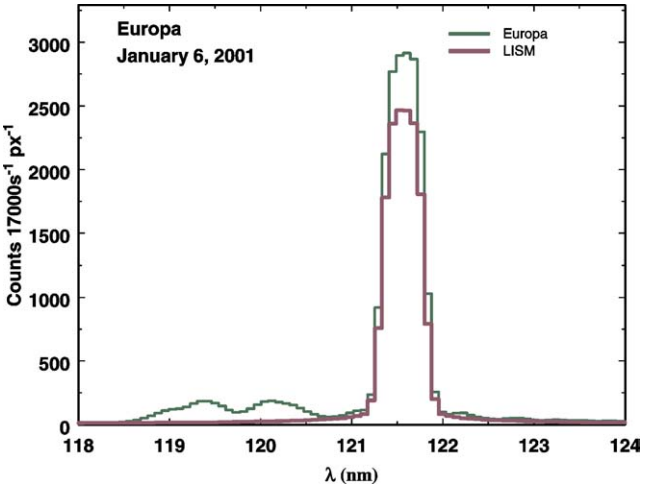

(e)

Fig. 2. Continued.

The first model step, the oxygen emission model, was developed by Don Shemansky. Atomic oxygen emission rates are based on experimental data acquired with P. Johnson (Johnson et al., 2003; Shemansky and Liu, in preparation). The rate coefficients for molecular oxygen are derived from experimental data acquired by Kanik et al. (2003) and are listed in Table 2. The jovian charged particle environment used in the model assumes a two-component electron environment: 40 e^- cm^3 with a temperature of 2.3×10^5 K (20 eV) plus a hot component with 4 e^- cm^3 and temperature of 2.3×10^6 K (200 eV). These values were selected to be effectively consistent with the quantities used by Hall and co-workers, to facilitate comparison of our data sets. Recent analysis of Galileo data indicates that the electron environment could be substantially different than these values (Frank et al., 2002), and potential effects on our analysis are discussed below. Modeling of the flux contributed by resonant scattering of solar photons at 1304 Å is also included in the oxygen emission model. The probability of emission given these processes and electron densities is listed in Table 3. The calculation of oxygen abundance from the emission flux is directly dependent on the values assumed for the electron density and energy, because they affect the rate coefficients, so different assumptions for the magnetospheric environment will yield different values for the abundance. (A derived abundance also depends on how the penetration of the electron flux propagates into Europa's atmosphere.

Table 3
Probability of emission given the charged particle environment and resonant scattering of solar photons for atomic oxygen

Wavelength (Å)	Probability of emission
1302.168	3.37E-07
1304.858	2.01E-07
1306.029	6.69E-08
Total	6.05E-07
1355.598	1.04E-07
1358.513	3.02E-08
1359.782	0.0
Total	1.342E-07

The presence of a model by Saur et al. (1998) allowed the derivation of an abundance based on our observations, but adjusted for our viewing geometry by the Saur model for electron density and energy within the atmosphere, with caveats, as discussed below.)

The second model step, the instrument simulation, includes all of the calibration factors determined for the UVIS instrument including the point spread function, wavelength scale, scattered light in the optics, and the instrument sensitivity as a function of wavelength. All values use the latest analysis of UVIS inflight calibration data.

A point source provides the best fit to the shape of the 1356 Å emission feature, consistent with a bound O_2 atmosphere not extending very far above the surface of Europa. On January 6, the shift in the feature due to Europa's offset from the center of the slit is best matched by the source being offset by 0.57 mr. The offset is calculated from the shift of the positions of the known emission source lines relative to their position in the UVIS spectrum, also well determined from calibration data. When the expected 0.37 mr pointing offset of the UVIS FUV relative to the ISS NAC boresight used to target the observation is incorporated, this offset puts the center of the point source on the unilluminated side of Europa (see Fig. 1a), consistent with the side that would be impacted by corotation plasma. The spectral shift of the 1304 Å emission feature is 0.32 mr, putting the source on the illuminated side of Europa. Since UVIS is a spectrograph the shift of 1304 relative to 1356 is unambiguously determined. Since a portion of the emission is due to resonantly scattered solar photons it is not surprising to find this emission strongest on the illuminated side.

Once the 1356 Å feature has been fit, the abundance of molecular oxygen and its contribution to the 1304 Å fea-

ture are calculated. The remaining flux at 1304 Å is then attributed to the resonant scattering of sunlight by atomic oxygen and electron excitation ($e^- + O$). A point source component plus an assumed filled field extended atomic oxygen atmosphere are required to best fit the 1304 Å spectral feature. This division is somewhat subjective and the allocation of flux to the point source vs. the extended source could be off by as much as 35%. With this caveat, our spectrum is best fit by including the presence of $\sim 2\%$ atomic O in the point source bound atmosphere (i.e. 98% O_2) plus the extended tenuous component. Although no unambiguous detection of atomic oxygen was reported by Hall et al. (1995, 1998) their observation geometry would not have lent itself to distinguishing O from O_2. Europa subtends a much smaller fraction of the UVIS pixel than the GHRS HST IFOV, thus more of the surrounding space is included, enabling our detection of the extended atomic oxygen.

Fig. 3a shows the distribution of oxygen in the January 6 data set as a function of spatial row. The 1356 Å feature is sharply peaked at pixel 32. The diffuse 1304 Å feature persists across all the illuminated spectral pixels and is detectable in rows 28, 29, and 30. This spatial region encompasses Io's torus (see Fig. 1a). Fig. 3b shows the distribution of the oxygen in the January 12 data set. Most of the January 12 data set was collected at the ansa of Europa's orbit, free of Io torus emissions We postulate that the O_2 is indeed bound to Europa, however the atomic oxygen has both a loosely bound component showing the spectral character of a point source and a diffuse component which overfills a single pixel. The low spatial resolution hampers our ability to judge the size of the diffuse extended atmosphere, and any potential asymmetries (such as suggested by Burger and Johnson (2004) for Europa's sodium atmospheric component). We estimate that it is approximately equal to one pixel in extent, or ~11,000 km at Cassini's range.

Table 4 compares the Cassini observations to the HST observations. The error bars on the Cassini measurements are $+/- \sim 15\%$. The flux for the HST observations was taken from Hall et al. (1998) and converted to the irradiance that would have been detected by UVIS at Cassini's range. The January 12 Cassini flux has been adjusted for the range difference between the 6th and the 12th of January. The HST observed Europa at the east and west elongations of its orbit, while the Cassini observations were on the solar side and anti-solar side of Jupiter. Hall et al. (1998) derived a molecular oxygen vertical column density of $(2.4–14) \times 10^{14}$ cm^{-2}. Our molecular oxygen abundances fall within this range.

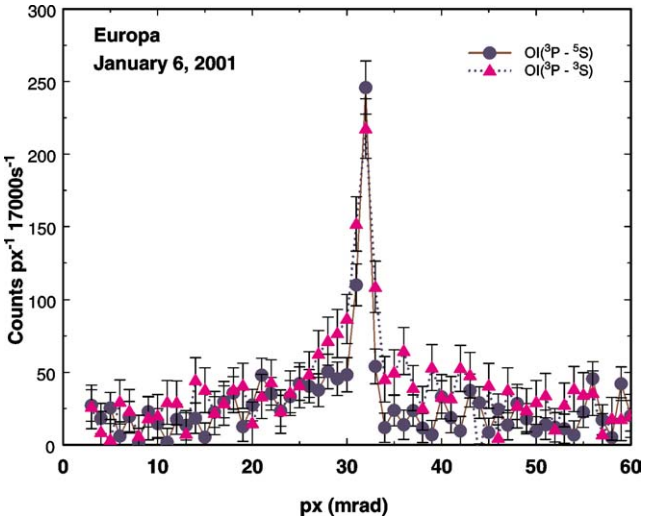

(a)

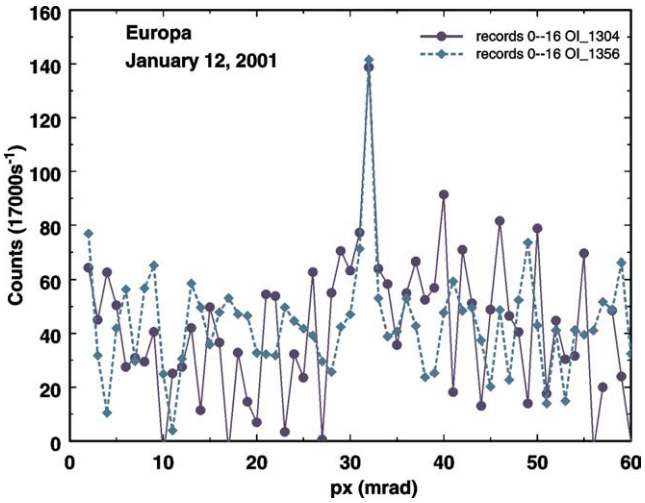

(b)

Fig. 3. (a) This plot shows the distribution of the 1304 and 1356 Å oxygen emission in the January 6, 2001 data set along the slit spatial dimension. The 1356 Å feature is sharply peaked at the position of Europa. The diffuse 1304 Å feature source persists across all the illuminated spectral pixels and is detectable in row 28, which corresponds to the opposite side of Europa's orbit (see Fig. 1a). (b) The oxygen line emissions for the first 4.7 h of the January 12 data set are shown, along the slit spatial dimension as in panel (a). Most of the January 12 data set was collected near the ansa of Europa's orbit as seen from Cassini, illustrated in Fig. 1c(1). Both 1304 and 1356 Å are sharply peaked at Europa's position.

Table 4
Comparison of irradiance (photon/cm^2 s) measured by Cassini UVIS (attributed to a point source) to HST data. The HST flux has been adjusted to the Cassini range from Europa on January 6. The January 12 flux at Cassini has been adjusted for the difference in range relative to January 6

	Cassini		HST, adjusted to Cassini range		
	January 6	January 12	1994 trailing	1996 trailing	1996 leading
1304 Å observed flux	0.47	0.16	0.27	0.40	0.28
1356 Å observed flux	0.99	0.31	0.42	0.45	0.41
1356/1304 airglow ratio	2.1	1.9	2.2	1.3	2.1

Table 5
Measured and derived values for Europa's bound oxygen atmosphere, assuming a scale height of 196 km (for $T = 1000$ K)

	January 6	January 12
Total 1304 Å flux (photon/cm^2 s)	0.47	0.10
Total 1356 Å flux (photon/cm^2 s)	0.99	0.18
Range (km)	11.2×10^6	15.8×10^6
Total 1304 Å disk-averaged brightness (point source only, Rayleighs)	130	73
Total 1356 Å disk-averaged brightness (Rayleighs)	1440	540
[O_2] mean density (cm^{-3})	6.2×10^7	3.7×10^7
[O_2] column density (cm^{-2})	12.4×10^{14}	7.4×10^{14}
[O] mean density (cm^{-3})	1.5×10^6	0.85×10^6
O column density (cm^{-2})	3.1×10^{13}	1.7×10^{13}
[O]/[O] + [O2]	0.02	0.02
Diffuse extended atomic oxygen atmosphere density (cm^{-3})	31	12

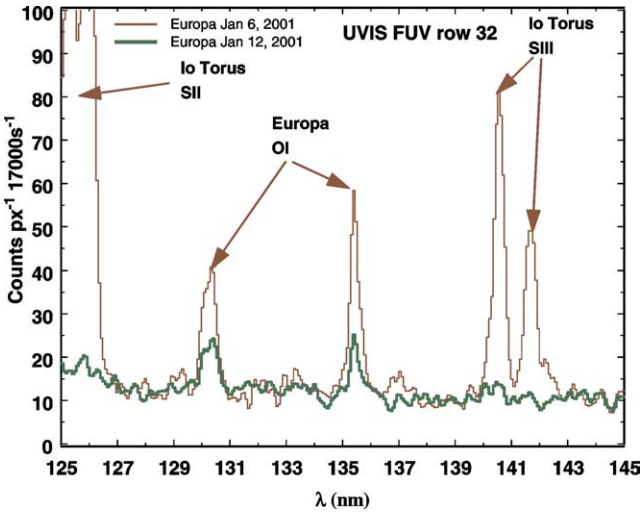

Fig. 4. This comparison of January 6 and January 12, 2001 exposures shows the flux from the later exposure reduced by a factor of ∼3. With Europa at the ansa of its orbit as seen from Cassini, Io's torus was not within the UVIS field of view on January 12.

Atomic and molecular oxygen abundances are tabulated in Table 5. These are derived values, based on the flux observed at the instrument. Assumptions that go into these derived values include the scale height of the atmosphere, and the electron energy and density. A change to any of these parameters will change these quantities, so if better data becomes available these quantities can be recomputed. It is important to note that actual in situ measurements of the electron environment simultaneous to the observations were not acquired by Cassini, which was well outside the magnetosphere at this time, thus these values will always be model-dependent.

Even with the adjustment for the range change, differences between the January 6 and January 12 data sets are apparent, as illustrated in Fig. 4. There is no plausible change in instrument performance that could explain these changes. Calculation of abundance based on uniform average flux gives us an oxygen abundance that differs by a factor of 3 between the two observation sets, however since the oxygen emission is dependent on the electron environment we postulate that these differences primarily reflect the difference in the viewing geometry.

In order to explore the variability due to viewing geometry we calculated the emission based on the electron environment modified by the presence of Europa's atmosphere as described by Saur et al. (1998). The Saur et al. model features a steady-state distribution of electron energies around Europa, with plasma flowing in on one side and creating a cavity on the other, producing nonuniform excitation of the oxygen. At the time of the January 12 observation UVIS was looking at the leading side of Europa, at a wake region depleted of electrons (a cavity formed by plasma flowing around Europa), depicted in Fig. 7 of Saur et al. (1998). We used the Saur and co-workers model for the electron distribution in the atmosphere to quantitatively derive the oxygen abundance. Our observations are qualitatively consistent with the Saur and co-workers model, however we estimate that just up to a factor of ∼1.6 difference in brightness can be attributed to the difference in leading vs. trailing side electron density and electron energy, vs. the 3× difference in flux we observed.

Using the Saur model and accounting for the viewing geometry we calculate molecular oxygen abundances of 7.4×10^{14} cm^{-2} on January 12 and 12.4×10^{14} cm^{-2} on January 6. These numbers are higher by as much as a factor of 2 than those considered by Saur and co-workers, so for this reason the Saur model may not be entirely appropriate for this derivation. The fact that the inferred atmospheric density is higher than that used by Saur and co-workers suggests that the geometric effect between January 6 and January 12 would be larger in a recalculated Saur model. For this reason the observed intensities on these two dates may well be compatible with a constant O_2 atmosphere. The timeline of the observations show no indication of a variable OI 1356 intensity on January 12 over an 11.4 h time interval, which leads us to discount an electron environment variability associated with the Io torus wobble. An increase in oxygen abundance between January 6 and January 12 might be indicative of a transient event, but the significant decrease between our two observations is harder to explain as a transient phenomenon. The most likely explanation is a change in the plasma environment such as reported by Frank et al. (2002). Electron densities can be estimated from their ion densities and may be 3 to 4 times the values we have used.

4.3. Europa's torus

From the UVIS data one cannot identify an atomic or molecular oxygen torus around Europa's orbit. We do see an extended atomic oxygen atmosphere at Europa. The density of oxygen in Europa's extended atmosphere is 12 to 31 atoms per cm^3, at the points in time and space that Cassini

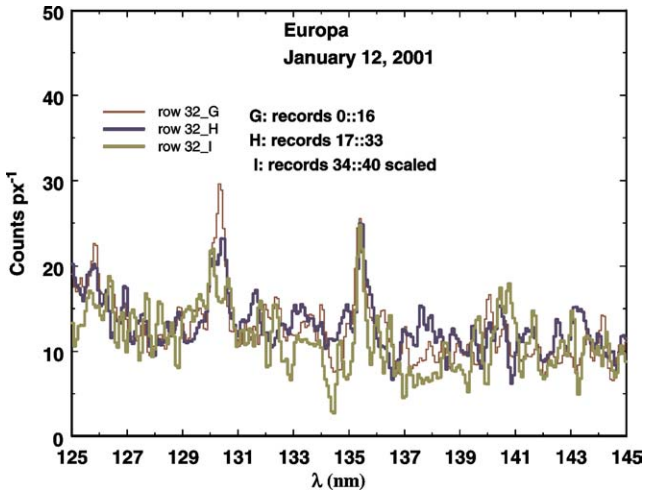

Fig. 5. The 11.4 h data set for January 12 has been divided into far side (integrations 0–16), ansa (integrations 17–33) and near side (integrations 34–40) segments, as Europa approached the spacecraft along its orbital track. The spectra show the 1356 Å emission feature is constant over this interval (which is longer than one jovian rotation), while the 1304 Å flux monotonically declines in intensity.

observations were acquired. We do not see atomic oxygen emission at other places in Europa's orbit that are distant from Europa. The spatial extent of the atomic oxygen is shown in Figs. 3a and 3b. The spatially extended nature of the 1304 Å emission across pixels 27 to 33 in the January 6 data (Fig. 3a) could be attributed to the oxygen in Io's torus. In the January 12 data set the pathlength through the purported torus increases by a factor of 6 from the beginning to the end of the observation. As shown in Fig. 5, while the flux at 1356 Å holds steady the flux at 1304 Å decreases monotonically—the opposite of expectation as the pathlength increases if there were a torus. As noted earlier the unchanging nature of the 1356 Å flux over one jovian rotation is indicative of the uniformity of the excitation process over the Io torus wobble.

In order to put upper bounds on oxygen density in Europa's postulated torus we analyzed data from one of the outbound UVIS Io torus observations acquired in February 2001. This observation was designed with the UVIS slit centered on Jupiter and oriented parallel to Jupiter's equator, shown in Fig. 6a. This data set had full spectral and spatial resolution, and a total integration time of $\sim$ 28 h. During the observation the boresight was slewed slowly from north to south every 30 min, such that the total integration time in a particular direction was approximately 7 h. Fig. 6b shows a 3-dimensional plot of the UVIS data. In the data illustrated in Fig. 6b, Io's orbit extends $\sim$12 rows from Jupiter (to row 21 and row 43, Jupiter in row 32) and Europa's orbit extends another 6 rows. Atomic oxygen in the Io torus appears as expected, as emission extending from row 21 to row 43. If there were a Europa torus containing atomic oxygen it would appear in rows 14 to 15 and 48 to 49. As shown in Fig. 6c, there is no atomic oxygen emission at the position of the Europa ansa. We thus conclude that oxygen is not a contributor to the torus identified by Mauk et al. (2003) at 9.5 R_J at levels detectable by UVIS. The density that UVIS could detect in a 7 h integration is $\sim$ 8 atoms/cm^3, a factor of 5 less than the value postulated by Mauk and co-workers for a torus radius of 2 R_J.

The atomic oxygen in the Europa's extended atmosphere is subject to ionization and loss, from photoionization, charge exchange, and electron dissociation. The rate of ionization from these three processes is $\sim 1.6 \times 10^{-6}$ s^{-1}, thus the lifetime for an oxygen atom in Europa's exosphere is estimated to be 7.2 days. In theory enough oxygen atoms are lost from Europa's atmosphere to account for the total number required by Mauk and co-workers, as neutral species distributed in the magnetosphere. The distribution however would have to be over a torus-like object at least 5 R_J in diameter, in order to obtain a null detection by UVIS.

4.4. Hydrogen Lyman alpha feature

Another likely species in a Europa torus is hydrogen (e.g., Shematovich et al., in preparation). We analyzed the spatial distribution of the Lyman alpha (HLya) excess emission (greater than the LISM signature) in our January 6 and 12 data to investigate the hydrogen distribution.

In the January 6 data set an excess signal of HLya was detected, associated with Europa. On January 12 a marginal excess was observed, at least a factor of 8 less intense. Spatial distribution of this feature on both dates is complex, and indicates that HLya may be contaminated with another emission. The analysis of this feature is incomplete. Further discussion is deferred to a following paper.

5. Other satellite observations

UVIS participated in a number of satellite observations with the other Cassini remote sensing instruments. Unfortunately most of the observations in the week prior to closest approach, when the spacecraft was relatively close to Jupiter and the satellites were at low phase angles, were lost due to a spacecraft reaction wheel anomaly. In spite of this setback very good results were achieved for Io, reported in (Hendrix et al., in preparation).

Ganymede and Callisto were observed but not detected successfully because the instrument slit configuration selected for these observations was not (with hindsight) the best choice. This was especially disappointing for Ganymede, known to also have a bound oxygen atmosphere (Hall et al., 1998) and escaping hydrogen (Barth et al., 1997), as it would have been interesting to compare these observations to the Cassini results.

5.1. Summary and conclusions

Cassini UVIS observations of Europa confirm the detection by HST of a bound O_2 atmosphere. We also detect

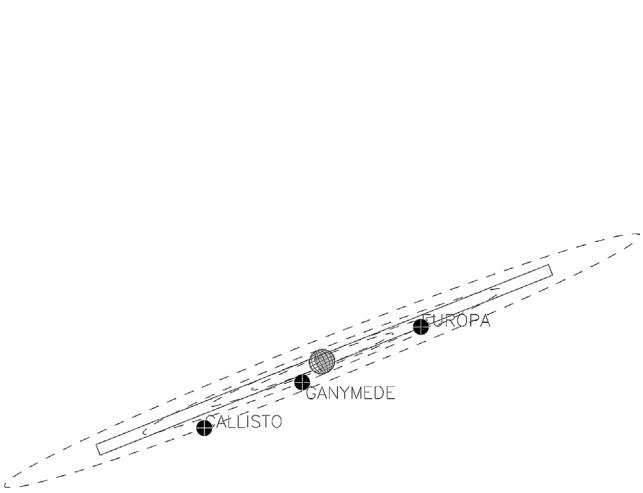

(a)

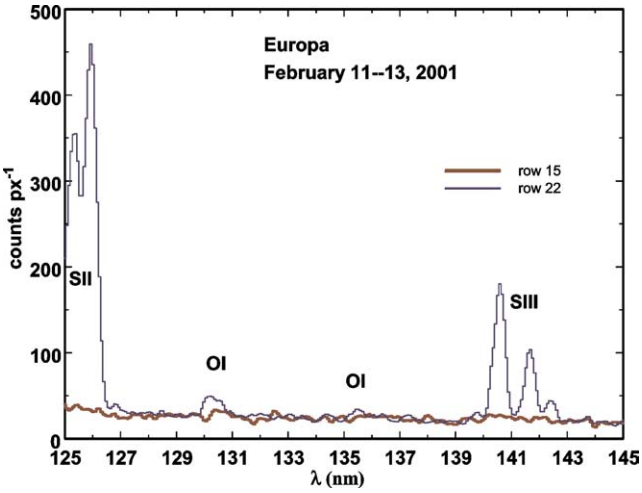

(c)

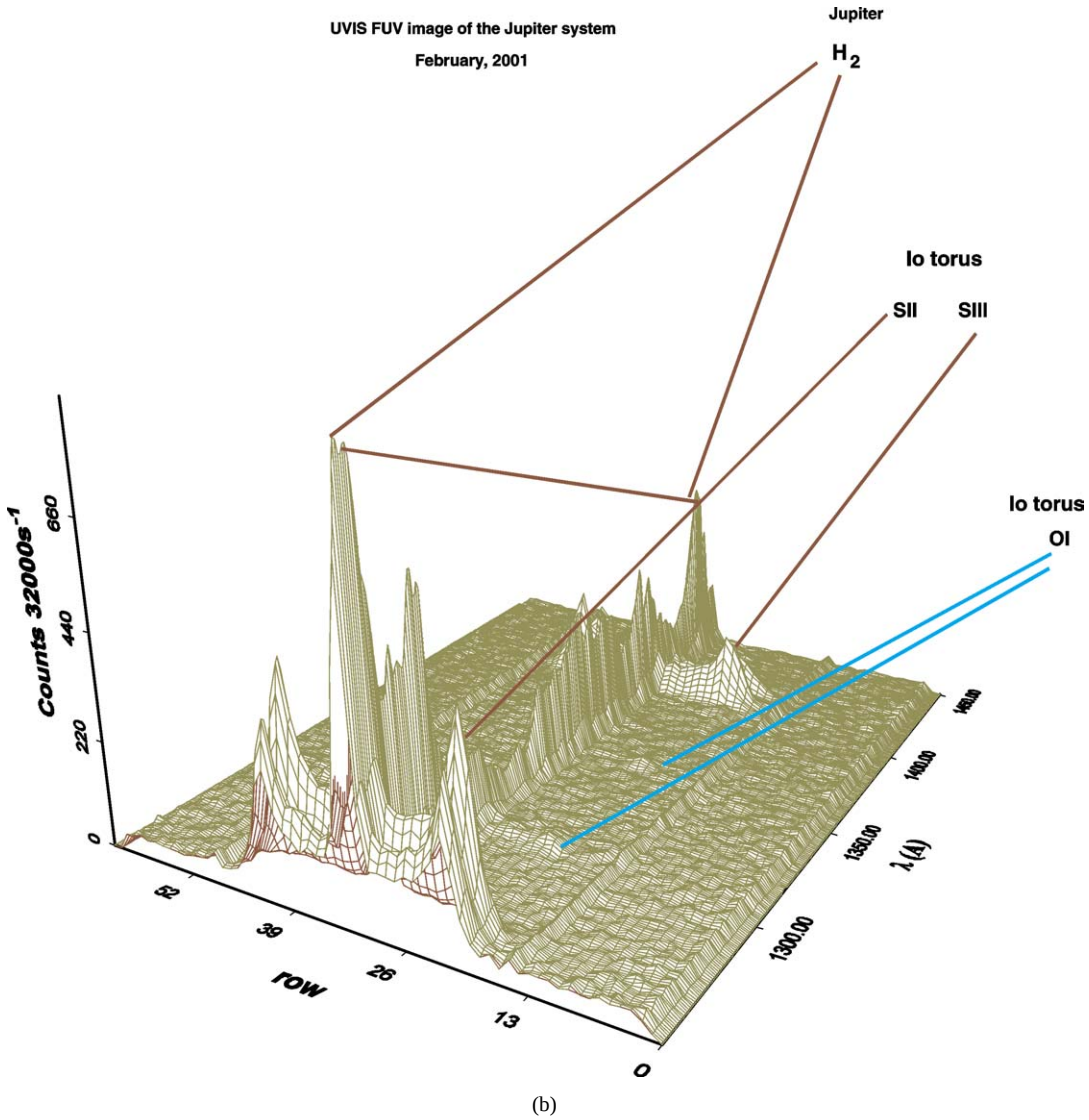

(b)

Fig. 6. (a) Outbound Jupiter system data collected February 11–13, 2001, was analyzed to search for the presence of a Europa oxygen torus. In these observations the slit was oriented perpendicular to Jupiter's spin axis. Data was collected for 28 h however the slit was slewed from north to south by 4 slit widths in a 30 min repeat cycle, thus actual integration time was ∼7 h. (b) This image of the Jupiter system is a subset of the FUV spectrum including the location of the Europa orbit and shows the Io torus and planetary emission. There is no detectable signature of a Europa oxygen torus. (c) The Io torus ansa spectrum at row 22 is shown compared to the Europa orbit ansa at row 15. Oxygen lines are not detectable in the Europa row.

atomic oxygen, partially bound to Europa (thus showing up as a point source in our data) and partially dispersed in an extended atmosphere.

Strong observed variability in emission in our two data sets (January 6 and January 12) appears to be attributable only in part to observation geometry, according to comparison to the Saur and co-workers model. Between Cassini and HST Europa has been observed at 4 different locations in its orbit. HST detected a factor of 2 difference in flux from the trailing side between 1994 and 1996, and between the leading and trailing sides in 1996 (Hall et al., 1995, 1998). Variability of emission brightness over a 6.5 h interval was also reported in the 1999 HST observations (McGrath et al., 2000, 2004). The variability of the signal from Europa's atmosphere beyond the amount attributable to viewing geometry appears to be caused by temporal variability in the source or in the electron environment, and promises to be an intriguing investigation in the future.

The detection of atomic oxygen as an extended atmosphere adds a new observational constraint to models of the erosion of Europa's surface and life cycle of its atmosphere in the jovian environment, such as those developed by Saur et al. (1998), Shematovich and Johnson (2001), or Shematovich et al. (in preparation). A calculation of the rate of delivery of atomic oxygen into the magnetosphere from Europa implies that the total population of neutrals in the extended region around the Europa orbit, compatible with the Mauk and co-workers results, could be maintained. This number quantity of OI must however be distributed over a 5 R_J or larger radial region at 9.5 R_J in order to be compatible with the nondetection of a torus signal by UVIS.

The distribution of hydrogen in Jupiter's magnetosphere has appeared in UVIS data with unexpected complexity. A future paper will discuss the source and processes governing the hydrogen distribution.

Acknowledgments

We extend special thanks to Ian Stewart for providing the LISM spectrum from Cassini cruise observations; Joe Ajello, Larry Esposito, Bill McClintock, Joachim Saur, Darrell Strobel, and Andrew Steffl for helpful discussions, and Janet Tew for invaluable support with data reduction. This work was partially supported by the Jet Propulsion Laboratory, California Institute of Technology, under a contract with the National Aeronautics and Space Administration.

References

Barth, C.A., Hord, C.W., Stewart, A.I.F., Pryor, W.R., Simmons, K.E., McClintock, W.E., Ajello, J.M., Naviaux, K.L., Aiello, J.J., 1997. Galileo ultraviolet spectrometer observations of atomic hydrogen in the atmosphere of Ganymede. Geophys. Res. Lett. 24, 2147–2150.

Burger, M.H., Johnson, R.E., 2004. Note: Europa's neutral cloud: Morphology and comparisons to Io. Icarus 171, 557–560.

Cheng, A.F., Haff, P.K., Johnson, R.E., Lanzerotti, L.J., 1986. Interactions of planetary magnetospheres with icy satellite surfaces. In: Burns, J.A., Matthews, M.S. (Eds.), In: Satellites. Univ. of Arizona Press, Tucson, AZ, pp. 403–436.

Esposito, L.E., Barth, C.A., Colwell, J.E., Lawrence, G.M., McClintock, W.E., Stewart, A.I.F., Keller, H.U., Korth, A., Lauche, H., Festou, M.C., Lane, A.L., Hansen, C.J., Maki, J.N., West, R.A., Jahn, H., Reulke, R., Warlich, K., Shemansky, D.E., Yung, Y.L., 2003. The Cassini Ultraviolet Imaging Spectrograph investigation. Space Sci. Rev. In press.

Frank, L.A., Paterson, W.R., Khurana, K.K., 2002. Observations of thermal plasmas in Jupiter's magnetotail. J. Geophys. Res. 107 (A1), 1003, 10.1029/2001JA000077.

Hall, D.T., Strobel, D.F., Feldman, P.D., McGrath, M.A., Weaver, H.A., 1995. Detection of an oxygen atmosphere on Jupiter's moon Europa. Nature 373, 677–679.

Hall, D.T., Feldman, P.D., McGrath, M.A., Strobel, D.F., 1998. The far-ultraviolet oxygen airglow of Europa and Ganymede. Astrophys. J. 499, 475–481.

Ip, W.H., 1996. Europa's oxygen exosphere and its magnetospheric interaction. Icarus 120, 317–325.

Johnson, P.V., Kanik, I., Shemansky, D.E., Liu, X., 2003. Electron-impact cross sections of OI. J. Phys. B. 36, 1.

Johnson, R.E., 1996. Sputtering of ices in the outer Solar System. Rev. Modern Phys. 68, 305–312.

Johnson, R.E., Quickenden, T.I., 1997. Photolysis and radiolysis of water ice on outer Solar System bodies. J. Geophys. Res. Planets 102, 10,985–10,996.

Johnson, R.E., Lanzerotti, L.J., Brown, W.J., Armstrong, T.P., 1981. Erosion of Galilean satellites by jovian magnetospheric particles. Science 212, 1027–1030.

Kanik, I., Noren, C., Makarov, O.P., Vatippalle, P., Ajello, J.M., Shemansky, D.E., 2003. Electron impact dissociative excitation of O_2: Absolute emission cross sections of the OI (130.4 nm) and OI (135.6 nm) lines. J. Geophys. Res. 108, 12-1–12-10.

Lagg, A., Krupp, N., Woch, J., Williams, D.J., 2003. In-situ observations of a neutral gas torus at Europa. Geophys. Res. Lett. 30, 1556–1559.

Mauk, B.H., Mitchell, D.G., Krimigis, S.M., Roelof, E.C., Paranicas, C.P., 2003. Energetic neutral atoms from a trans-Europa gas torus at Jupiter. Nature 421, 920–922.

McClintock, W.E., Lawrence, G.M., Kohnert, R.A., Esposito, L.W., 1992. Optical design of the Ultraviolet Imaging Spectrograph for the Cassini mission to Saturn. SPIE 1745, 26–38.

McGrath, M.A., Feldman, P.D., Strobel, D.F., Retherford, K., Wolven, B., Moos, H.W., 2000. HST/STIS ultraviolet imaging of Europa. Bull. Am. Astron. Soc. 31, 1056. Abstract.

McGrath, M.A., Lellouch, E., Strobel, D.F., Feldman, P.D., Johnson, R.E., 2004. Satellite Atmospheres. In: Bagenal, F., Dowling, T., McKinnon, W. (Eds.), Jupiter: The Planet, Satellites and Magnetosphere. Cambridge University Press, Cambridge.

Porco, C.C., West, R.A., McEwen, A., Del Genio, A.D., Ingersoll, A.P., Thomas, P., Squyres, S., Dones, L., Murray, C.D., Johnson, T.V., Burns, J.A., Brahic, A., Neukum, G., Veverka, J., Barbara, J.M., Denk, T., Evans, M., Ferrier, J.J., Geissler, P., Helfenstein, P., Roatsch, T., Throop, H., Tiscareno, M., Vasavada, A.R., 2003. Cassini imaging of Jupiter's atmosphere, satellites, and rings. Science 299, 1541–1547.

Saur, J., Strobel, D.F., Neubauer, F.M., 1998. Interaction of the jovian magnetosphere with Europa: Constraints on the neutral atmosphere. J. Geophys. Res. 103, 19,947–19,962.

Shematovich, V.I., Johnson, R.E., 2001. Near-surface oxygen atmosphere at Europa. Adv. Space Res. 27, 1881–1888.

Shi, M.R., Baragiola, A., Grosjean, D.E., Johnson, R.E., Jurac, S., Schou, J., 1995. Sputtering of water ice surfaces and the production of extended neutral atmospheres. J. Geophys. Res. Planets 100, 26,387–26,395.